RESEARCH ARTICLE

Simulation and Experimental Research on Active Suspension System With Time-Delay Feedback Control

YANG NAN[ID], SUJUAN SHAO, CHUANBO REN[ID], KAIWEI WU[ID], YAJIE CHENG, AND PENGCHENG ZHOU

School of Transportation and Vehicle Engineering, Shandong University of Technology, Zibo 255049, China

Corresponding author: Sujuan Shao (ssjsdut@sdut.edu.cn)

ABSTRACT A 2-DOF vehicle active suspension system model with time-delay feedback control is established. The stability region of the time-delay active suspension system is obtained by using the Routh-Hurwitz stability criterion and polynomial discriminant theory. The multi-objective optimization function is established taking into account vehicle ride comfort, driving safety, and handling stability, and the optimal feedback parameters are obtained by the particle swarm optimization(PSO) algorithm. The vibration characteristics of active suspension systems with time-delay under different road excitations are studied through experiments and simulations and then compared with passive uncontrolled suspension and active suspension based on LQR. The experimental results show that the sprung mass acceleration(SMA) of the active suspension system with optimal time-delay feedback control under harmonic excitation is reduced by 58.02% and 39.18% compared to the passive suspension system and the LQR active suspension system, respectively. Meanwhile, the sprung mass acceleration of the active suspension system with optimal time-delay feedback control under random excitation has a 69.56% and 35.50% reduction compared to the passive suspension system and the LQR active suspension system, respectively. The performance of active suspension controlled by time-delay feedback is better than that of passive suspension and LQR active suspension in numerical study and experiment. Moreover, the experimental and simulation results show good consistency, which proves the reliability of the experimental results.

INDEX TERMS Active suspension, experiment, stability, time-delay, vibration.

I. INTRODUCTION

This work was supported in part by National Natural Science Foundation of China When the vehicle is in motion, frequent vertical vibration caused by road roughness has been recognized as a serious hazard to vehicle drivers [1], [2], [3]. The application of lightweight technology in modern automobile bodies makes vehicles more sensitive to vibration, which may shorten the service life of some components due to premature fatigue failure [4]. More importantly, people's vibration sensory organs are all over the body. When the vibration is strong, it will cause disorders in the nervous

The associate editor coordinating the review of this manuscript and approving it for publication was Hassen Ouakad[ID].

system and internal organs [5], and affect the human cardio-vascular, digestive, nervous, urinary, and sensory systems [6]. Therefore, it is necessary to study the vehicle suspension system with better vibration damping performance.

Vehicle system dynamics is a study of vehicle power, fuel economy, handling stability, ride comfort, and passability. The performance of the suspension system directly affects handling stability and ride comfort, so it is necessary to study active suspension. Active suspension with active or passive controllable components forms a closed-loop or open-loop control system, which reacts according to the motion state of the vehicle system and the change of external input [7]. Prassad and Mohan [8] proposed an adaptive air suspension system based on the LQR control strategy. In MATLAB,

the most commonly used PID controller and the LQR controller proposed in this paper are compared and analyzed for bump pavement, pothole pavement, and ISO standard random pavement. The performance of the adaptive air suspension system is evaluated experimentally on the vibration table. The experimental results show that the sprung mass acceleration of the adaptive air suspension system decreases by about 30% under the random vibration of 5 Hz ~ 20 Hz, which indicates that the controller is effective for random vibration input. Robert et al. [9] analyzed the performance of a model-free intelligent fuzzy controller based on an intelligent fuzzy controller. A model-free intelligent adaptive fuzzy controller for active suspension is proposed. The Fuzzy controller can predict and control the performance of active suspension well. The simulation results show that the non-flexible fuzzy control is superior to the conventional controller in terms of body displacement and acceleration. However, in all control systems, there is an inevitable time lag phenomenon in the signals acquisition and transmission of sensors, processing of signals by the operators, and the actuation of actuators, which is called time-delay [10]. Olgac and Holm-Hansen [11] introduced the time-delay feedback control into the dynamic absorber for the first time, formed the time-delay resonator, and applied it to the vibration control of the main system under harmonic excitation. The results show that the vibration of the main system is eliminated by selecting appropriate delay feedback control parameters.

When time-delay is added to the suspension system, on the one hand, the time delay will not only reduce the control accuracy but also lead to the loss of stability and the occurrence of bifurcation chaos [12]. On the other hand, a reasonable selection of feedback gain and time-delay can effectively improve the control performance of the suspension system, so the stability of the system when the time-delay is added should be ensured first. Taffo et al. [13] studied the stability switch and bifurcation of a two-degree-of-freedom nonlinear 1/4 vehicle with time-delay feedback. Qi et al. [14] established a time-delay feedback control strategy and mathematical model using pitch signals based on the mechanical model of the binary airfoil, carried out stability analysis of the system without and with time-delay, and obtained the time-delay stability boundary. Ye et al. [15] derived the dynamic model of the time-delay antilock braking system, obtained the stability region of the time-delay and the critical delay algorithm of the antilock braking system using the generalized Sturm criterion, and finally verified the effectiveness of the proposed critical time-delay algorithm through numerical simulation. Shao et al. [16] used the multi-scale dimensional normalized mathematical model for analytical calculation, and a new method for studying the stability of nonlinear time-delay systems is derived, finally, verified by numerical simulation. Zhou et al. [17] studied the nonlinear dynamics of a vehicle system with structural nonlinear unilateral vibration and obtained different paths to chaos through numerical analysis. Chen et al. [18] analyzed the dynamic
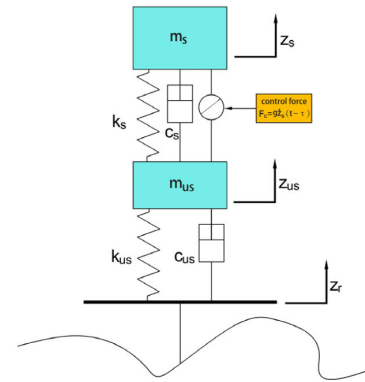

FIGURE 1. 2 DOF vehicle suspension control.

characteristics of time-delay semi-active suspension and on the basis of the simulations, a good damping effect consistent with the simulation results was obtained by a 1/4 model bench experiment. Vyhlída et al. [19] improved the existing method of approximating the load motion by the pendulum motion and proposed several nonlinear time-delay algorithms to deal with the load vibration problem suspended on a fixed base (e.g. a vertical crane), finally, the proposed time-delay feedback method was experimentally verified on the experimental device. Yan et al. [20] used the state change method to design the time-delay compensation control law, and the simulation shows that the control law can ensure the stability of the system and improve the damping performance, they built an experimental platform and finally obtained a credible result with an error within 15%.

Based on the above research, this paper combines theory and experiment to study the dynamic characteristics of the 2-DOF suspension model considering the influence of time-delay, and adds LQR optimal control as a control group while comparing time-delay feedback control with passive suspension in numerical simulation and experiment to further verify the superiority and effectiveness of time-delay feedback control on suspension performance improvement.

II. DYNAMIC MODEL OF VEHICLE ACTIVE SUSPENSION
A. MODEL ESTABLISHMENT
To facilitate the analysis of the effect of active suspension on vehicle vibrations (mainly vertical vibration) [21], assume that: 1) The vehicle is symmetrical to its longitudinal axis; 2) The impact between the front and rear parts of the vehicle is ignored; 3) The vertical dynamics of the tire can be simply equated to a spring and a damping mechanism, and then the 2-DOF dynamic model as shown in Fig.1 can be established.

m_s and m_{us} are sprung mass and unsprung mass, respectively. k_s is suspension stiffness; k_{us} is tire stiffness; c_s is suspension damping; c_{us} is tire damping; z_s and z_{us} are body displacement and tire displacement respectively; F_c is control force; τ is the delay of the suspension system; z_r is road surface displacement;

Using the second type of Laplace's equation, the dynamics equation of the suspension system can be obtained as follows:

$$
\begin{cases}
m_\text{s}\ddot{z}_\text{s} + k_\text{s}\,(z_\text{s} - z_\text{us}) + c_\text{s}\,(\dot{z}_\text{s} - \dot{z}_\text{us}) + F_\text{c} = 0 \\
m_\text{us}\ddot{z}_\text{us} + k_\text{s}\,(z_\text{us} - z_\text{s}) + c_\text{s}\,(\dot{z}_\text{us} - \dot{z}_\text{s}) + k_\text{us}\,(z_\text{us} - z_\text{r}) + \\
c_\text{us}\,(\dot{z}_\text{us} - \dot{z}_\text{r}) - F_\text{c} = 0
\end{cases}
\tag{1}
$$

The control force $F_c = g\dot{z}_s(t - \tau)$ is based on the body speed feedback, t is time, g is feedback gain, and τ is the time-delay of the suspension system. Table 1 shows the parameters of the suspension system experimental bench used in this paper.

TABLE 1. Experimental equipment model parameters.

Parameters	Value	Parameters	Value
m_s/kg	2.45	c_s/(N·s·m^{-1})	0-9
m_us/kg	1	c_us/(N·s·m^{-1})	5
k_s/(N·m^{-1})	980	g/(N·s·m^{-1})	-170-170
k_us/(N·m^{-1})	2500	τ/s	0-1

B. DIMENSIONLESS SYSTEM MODEL

To simplify the process of stability analysis, equation (1) is dimensionless, which can be expressed as:

$$
\begin{cases}
\overline{\ddot{z}}_\text{s} + (\overline{z}_\text{s} - \overline{z}_\text{us}) + \overline{c}_\text{s}\,(\overline{\dot{z}}_\text{s} - \overline{\dot{z}}_\text{us}) + \overline{F}_\text{c} = 0 \\
\overline{\ddot{z}}_\text{us} + \beta\,(\overline{z}_\text{us} - \overline{z}_\text{s}) + \beta\overline{c}_\text{s}\,(\overline{\dot{z}}_\text{us} - \overline{\dot{z}}_\text{s}) \\
+\beta\overline{k}\,(\overline{z}_\text{us} - \overline{z}_\text{r}) + \beta\overline{c}_\text{us}\,(\overline{\dot{z}}_\text{us} - \overline{\dot{z}}_\text{r}) \\
-\beta\overline{F}_\text{c} = 0
\end{cases}
\tag{2}
$$

In (2), $\overline{z}_\text{s}, \overline{\dot{z}}_\text{s}, \overline{\ddot{z}}_\text{s}$ are the dimensionless body lisplacement, velocity, and acceleration; $\overline{z}_\text{us}, \overline{\dot{z}}_\text{us}, \overline{\ddot{z}}_\text{us}$ are he dimensionless tire displacement, speed, and acceleration; $\overline{z}_\text{r}, \overline{\dot{z}}_\text{r}$ are the dimensionless road displacement and speed. ther dimensionless parameters are as follows: $\overline{t} = \sqrt{\frac{k_\text{s}}{m_\text{s}}}t$, $\overline{F}_\text{c} = \overline{g}\overline{\dot{z}}_\text{s}(\overline{t} - \overline{\tau})$, $\overline{c}_\text{s} = \frac{c_\text{s}}{\sqrt{k_\text{s}m_\text{s}}}$, $\overline{c}_\text{us} = \frac{c_\text{us}}{\sqrt{k_\text{s}m_\text{s}}}$, $\beta = \frac{m_\text{s}}{m_\text{us}}$, $\overline{g} = \frac{g}{\sqrt{k_\text{s}m_\text{s}}}$, $\overline{k} = \frac{k_\text{us}}{k_\text{s}}$, $\overline{\tau} = \sqrt{\frac{k_\text{s}}{m_\text{s}}}\tau$, $\overline{F}_\text{c} = \overline{g}\overline{\dot{z}}_\text{s}(\overline{t} - \overline{\tau})$ is the dimensionless time-delay control force.

For ease of reading, (2) is simplified a

$$
\begin{cases}
\ddot{z}_\text{s} + (z_\text{s} - z_\text{us}) + c_\text{s}\,(\dot{z}_\text{s} - \dot{z}_\text{us}) + F_\text{c} = 0 \\
\ddot{z}_\text{us} + \beta\,(z_\text{us} - z_\text{s}) + \beta c_\text{s}\,(\dot{z}_\text{us} - \dot{z}_\text{s}) + \beta k\,(z_\text{us} - z_\text{r}) + \\
\beta c_\text{us}\,(\dot{z}_\text{us} - \dot{z}_\text{r}) - \beta F_\text{c} = 0
\end{cases}
\tag{3}
$$

Considering the vehicle suspension performance index and ride comfort index comprehensively, the state space equation is defined as

$$
\begin{cases}
\dot{X} = AX + BU + EW(t) \\
Y = CX + DU + FW(t)
\end{cases}
\tag{4}
$$

where $X = [z_\text{s}, \dot{z}_\text{s}, z_\text{us}, \dot{z}_\text{us}]^\text{T}$ is the state vector; $Y = [\ddot{z}_\text{s}, \ddot{z}_\text{us}, z_\text{s} - z_\text{us}, z_\text{us} - z_\text{r}]^\text{T}$ is the output vector; the timedelay vector is $U = [z_\text{s}(t - \tau), \dot{z}_\text{s}(t - \tau), z_\text{us}(t - \tau), \dot{z}_\text{us}(t - \tau)]^\text{T}$;

$W(t) = [z_\text{r}, \dot{z}_\text{r}]^\text{T}$ is the excitation vector of the road surface. From what has been discussed above, the coefficient matrix of the system is

$$
A = \begin{bmatrix}
0 & 1 & 0 & 0 \\
-1 & -c_\text{s} & 1 & c_\text{s} \\
0 & 0 & 0 & 1 \\
\beta & \beta c_\text{s} & -\beta(1+k) & -\beta(c_\text{s} + c_\text{us})
\end{bmatrix}
\tag{5}
$$

$$
B = \begin{bmatrix}
0 & 0 & 0 & 0 \\
0 & -g & 0 & 0 \\
0 & 0 & 0 & 0 \\
0 & \beta g & 0 & 0
\end{bmatrix}
\tag{6}
$$

$$
C = \begin{bmatrix}
-1 & -c_\text{s} & 1 & c_\text{s} \\
\beta & \beta c_\text{s} & -\beta(k+1) & -\beta(c_\text{s} + c_\text{us}) \\
1 & 0 & -1 & 0 \\
0 & 0 & 1 & 0
\end{bmatrix}
\tag{7}
$$

$$
D = \begin{bmatrix}
0 & -g & 0 & 0 \\
0 & \beta g & 0 & 0 \\
0 & 0 & 0 & 0 \\
0 & 0 & 0 & 0
\end{bmatrix}
\tag{8}
$$

$$
E = \begin{bmatrix}
0 & 0 \\
0 & 0 \\
0 & 0 \\
\beta k & \beta c_\text{us}
\end{bmatrix}
\tag{9}
$$

$$
F = \begin{bmatrix}
0 & 0 \\
\beta k & \beta c_\text{us} \\
0 & 0 \\
-1 & 0
\end{bmatrix}
\tag{10}
$$

The parameters of the Experimental equipment model can be transformed into dimensionless parameters as shown in Table.2.

TABLE 2. Dimensionless model parameters.

Parameters	Value	Parameters	Value
β	2.45	c_us	0.102
τ	0-20	c_s	0-0.18
k	2.55	g	-3.5-3.5

III. STABILITY ANALYSIS
A. STABILITY ANALYSIS METHOD

According to the hysteretic differential equation theory, the characteristic equation of the system is

$$
\det(sI - A - Be^{-s\tau}) = 0
\tag{11}
$$

s is the characteristic root of the characteristic equation, by combining (5) and (6), the expansion polynomial of equation (11) can be obtained

$$
D(s, \tau) = P(s) + Q(s)e^{-s\tau}
\tag{12}
$$

For a given $\tau \geq 0$ system, the system is asymptotically stable if and only if the characteristic roots of the characteristic equation are on the negative half plane of the complex plane.

For any system, if any given $\tau \geq 0$ system is asymptotically stable, it is time-delay independent stability.

Theorem 1: A system is time-delay independent stability if and only if the following two conditions are met.

Condition 1. When $\tau = 0$ the polynomial $D(s, 0)$ satisfies the Routh-Hurwitz stability criterion.

Condition 2. For any $\tau > 0$, the polynomial has no pure imaginary roots $s = j\omega_0$, where j is an imaginary unit and ω_0 is a real number.

Expand the characteristic polynomial of (12), where P(s) and Q(s) are polynomials of fourth and third-order real coefficients respectively:

$$P(s) = s^4 + p_3 s^3 + p_2 s^2 + p_1 s + p_0 \quad (13)$$
$$Q(s) = q_3 s^3 + q_2 s^2 + q_1 s \quad (14)$$

Among them,

$$\begin{cases} p_0 = \beta k \\ p_1 = \beta(c_{us} + c_s k) \\ p_2 = \beta + 1 + \beta k + \beta c_{us} c_s \\ p_3 = c_s + \beta c_s + \beta c_{us} \\ q_1 = \beta g k \\ q_2 = \beta c_{us} g \\ q_3 = g \end{cases} \quad (15)$$

For condition 1 the requirements of the Routh-Hurwitz stability criterion are as follows

$$\begin{cases} R_1 = p_3 + q_3 > 0 \\ R_2 = p_2 + q_2 > 0 \\ R_3 = p_1 + q_1 > 0 \\ R_4 = p_0 > 0 \\ R_5 = (p_3 + q_3)(p_2 + q_2)(p_1 + q_1) - (p_1 + q_1)^2 - \\ (p_3 + q_3)^2 p_0 > 0 \end{cases} \quad (16)$$

For condition 2 in order to determine whether $D(s, \tau) = 0$ has pure imaginary roots, it is simplified and $s = j\omega_0$ is substituted, then the real and imaginary parts of $P(j\omega_0)$ and $Q(j\omega_0)$ can be expressed as

$$\begin{cases} P_R(\omega_0) = \mathrm{Re}[P(j\omega_0)] \\ P_I(\omega_0) = \mathrm{Im}[P(j\omega_0)] \\ Q_R(\omega_0) = \mathrm{Re}[Q(j\omega_0)] \\ Q_I(\omega_0) = \mathrm{Im}[Q(j\omega_0)] \end{cases}$$

And then separate the real part and the imaginary part, bring Euler's formula $e^{-jw_0\tau} = \cos(w_0\tau) - j\sin(w_0\tau)$ into equation (12), then obtain

$$D(j\omega_0, \tau) = P_R(\omega_0) + jP_I(\omega_0) + [Q_R(\omega_0) \\ + jQ_I(\omega_0)](\cos(\omega_0\tau) - j\sin(\omega_0\tau)) = 0 \quad (17)$$

So both the real and imaginary parts are 0,

$$\begin{cases} P_R(\omega_0) + Q_R(\omega_0)\cos(\omega_0\tau) + Q_I(\omega_0)\sin(\omega_0\tau) = 0 \\ P_I(\omega_0) + Q_I(\omega_0)\cos(\omega_0\tau) + Q_R(\omega_0)\sin(\omega_0\tau) = 0 \end{cases}$$
$$(18)$$

substitute $\cos^2(w_0\tau) + \sin^2(w_0\tau) = 1$ into (18) and eliminating the trig functions, can get

$$P_R(\omega_0)^2 + P_I(\omega_0)^2 - [Q_R(\omega_0)^2 + Q_I(\omega_0)^2] = 0 \quad (19)$$

This is a polynomial without time-delay, make
$F(\omega_0) = P_R(\omega_0)^2 + P_I(\omega_0)^2 - [Q_R(\omega_0)^2 + Q_I(\omega_0)^2]$, so

$$F(w_0) = \omega_0^8 + b_1\omega_0^6 + b_2\omega_0^4 + b_3\omega_0^2 + b_4 \quad (20)$$

In this formula,

$$\begin{cases} b_1 = 2(-\beta - \beta k - \beta c_s c_{us} - 1) - g^2 + (c_s + \beta c_s + \beta c_{us})^2 \\ b_2 = (-\beta - \beta k - \beta c_s c_{us} - 1)^2 + 2\beta k + 2\beta g^2 k + 2(c_s \\ + \beta c_s + \beta c_{us}) \\ (-\beta c_{us} - \beta c_s k) - \beta^2 c_{us}^2 g^2 \\ b_3 = 2\beta k(-\beta - \beta k - \beta c_{us} c_s - 1) - \beta^2 g^2 k^2 \\ + (-\beta c_{us} - \beta c_s k)^2 \\ b_4 = \beta^2 k^2, \end{cases}$$

$D(j\omega_0, \tau) = 0$ have no pure imaginary root, if and only if the formula has no real solution [22].

So far, the discussion of condition 2 is transformed into a judgment of the situation of the root of (20). If (20) has no real root, the system does not have stability switching. When the time-delay is 0, the system is stable, then the system is stable at all time-delay. On the contrary, the system with time-delay equal to zero is unstable so any given time-delay is unstable. Using the generalized Sturm criterion, the discriminant sequence of polynomials is defined as the sequence formed by the order principal minor of their Bezout matrix [22], written as $[D_1(f), D_2(f), \ldots, D_8(f)]$, It is equal to the $[1, d_0, d_0d_1, d_1d_2, d_2d_3, d_3d_4, d_4d_5, d_5^2d_6]$, where

$$\begin{cases} d_0 = -b_1 \\ d_1 = 3b_1^2 - 8b_2 \\ d_2 = b_1^2 b_2 + 3b_1 b_3 - 4b_2^2 \\ d3 = -3b_1^3 b_3 + b_1^2 b_2^2 - 6b_1^2 b_4 + 14b_1 b_2 b_3 - 4b_2^3 + \\ \quad 16b_2 b_4 - 18b_3^2 \\ d4 = -b_1^2 b_2^2 b_3 - 18b_1 b_2 b_3^2 + 7b_1^2 b_3 b_4 + 12b_1 b_2^2 b_4 - \\ \quad 48b_2 b_3 b_4 + 4b_2^3 b_3 + 16b_1 b_4^2 + 27b_3^3 + 4b_1^3 b_3^2 - \\ \quad 3b_1^3 b_2 b_4 \\ d5 = -27b_1^4 b_4^2 + 18b_1^3 b_2 b_3 b_4 - 4b_1^3 b_3^3 - 4b_1^2 b_2^3 b_4 + \\ \quad b_1^2 b_2^2 b_3^2 + 144b_1^2 b_2 b_4^2 - 6b_1^2 b_3^2 b_4 - 80b_1 b_2^2 b_3 b_4 + \\ \quad 18b_1 b_2 b_3^3 - 192b_1 b_2 b_4^2 + 16b_2^4 b_4 - 4b_2^3 b_3^2 - \\ \quad 128b_2^2 b_4^2 + 144b_2 b_3^2 b_4 + 256b_4^3 - 27b_3^4 \\ d_6 = b_4 \end{cases}$$

B. STABILITY ANALYSIS

The parameter space is selected from the dimensionless model parameters

$$\Omega = \{(g, c_s) \,||g| < 3.5, 0 < c_s < 0.18\},$$

In order to obtain the final time-delay independent stability region, the stability region of the Routh-Hurwitz criterion can be obtained when condition.1 is satisfied, as shown in Fig.3.

Then, b_1, b_2, b_3, and b_4 in (20) were substituted into the sequence of Sturm discriminant, draws $d_i = 0 (i = 0, 1, \ldots, 6)$ in the parameter space, and the stability region was obtained by intersection with Fig.3, as shown in Fig.4. The discriminant sequence symbols are shown in Table.3. l and k are the numbers of terms that are not equal to 0 and the number of sign changes in the discriminant sequence respectively, l-$2k$ is the number of real roots. In the green approximately V-shaped region S1, S2 are all 4, $F(\omega_0) = 0$ has $0(\frac{8-2\times4}{2} = 0)$ real roots, and the system has no stability switching, which is a stable region with all time-delay. In the yellow area S3, S4, S5, and S6, $F(\omega_0) = 0$ has exactly $2(\frac{8-2\times2}{2} = 2)$ reciprocal positive real roots, that is, (12) has pure virtual roots, and the system stability can be changed at any time with the change of hysteresis, find the reciprocal positive real roots and the critical time-delay can be obtained by using (21)

$$\tau_{i,j} = \tau_0 + \frac{2j\pi}{\omega_0}, i = 1, 2, \ldots; j = 0, 1, \ldots \quad (21)$$

where ω_0 is the positive real root of (20), τ_0 is the initial critical delay, $\tau_{i,j}$ represents the j-th critical delay corresponding to the i-th positive real root.

Then determine the change direction of the real part of the characteristic root when τ changes, that is to determine its sign $S = \text{sgn}\left\{\text{Re}(\frac{ds(\tau)}{d\tau})\,|s = i\omega_0\right\}$. Meanwhile, by observing Fig.4, it can be seen that the time-delay independent stability region increases with the increase of c_s, it conforms to the law that damped c_s is the source of time-delay independent stability of the system [23].

Theorem 2: If $f(x)$ is an n-th order polynomial, the discriminant sequence is $[D_1(f), D_2(f), D_3(f), \ldots, D_8(f)]$, let l and k be the number of non-zero terms and the number of sign changes in the discriminant sequence sign table, respectively. When $D_1(f) \neq 0, D_m(f) = 0 (m > l)$, the following explanations are definitive:

① If $l - 2k = 0$, the system is time-lag independent stable, or unstable, this depends on whether the system is asymptotically stable or unstable when the time delay is 0.

② If $l - 2k > 0$, there are a finite number of stability switching points for the system as the time delay increases, finally, it is unstable. To verify the validity of the above conclusions, We select the parameters for the simulation.

Example: $g = 0.1, c_s = 0.03$, this point is taken from the S4 area. The polynomial $F(\omega_0)$ has two distinct real roots at

this point, $\omega_1 = 0.7981$, $\omega_2 = 0.8702$, and satisfies $\dot{F}(\omega_1) < 0$, $\dot{F}(\omega_2) > 0$. The corresponding critical time-delays are $\tau_{1,0} = 0.6794, \tau_{1,1} = 1.7392, \ldots, \tau_{2,0} = 0.4527, \tau_{2,1} = 1.1012, \tau_{2,2} = 1.4206, \ldots$

Order them $\tau_{2,0} < \tau_{1,0} < \tau_{2,1} < \tau_{2,2} < \tau_{1,1} < \ldots$

Because $\dot{F}(\omega_1) < 0$, S=-1, So the real part of the characteristic root changes from positive to negative when the time delay crosses $\tau_{1,j}(j = 0, 1, \ldots)$, the system change from unstable to stable. The situation is reversed for $\dot{F}(\omega_2) > 0$. So the system is asymptotically stable when $\tau \in [0, \tau_{2,0})$, as shown in Figure 2(a), When $\tau \in [\tau_{2,0}, \tau_{1,0}]$, the system is unstable, as shown in Figure 2(b), When $\tau \in [\tau_{1,0}, \tau_{2,1}]$, the system becomes stable again, as shown in Figure 2(c). The simulation results verify the correctness of the theoretical analysis.

IV. OPTIMIZATION OF FEEDBACK PARAMETERS

A. ESTABLISHMENT OF OBJECTIVE FUNCTION

According to the recommendations of ISO-2631-1, the sprung mass acceleration(SMA) $\ddot{z}_s$ mainly determines the ride comfort quality of the vehicle, the dynamic tyre displacement(DTD) $z_{us} - z_r$ determines the ability of the tyres to adhere to the ground and the value of the suspension working stroke(SWS) $z_s - z_{us}$ needs to ensure that the vehicle will not appear the impact of the limit block. These three weight coefficients are determined subjectively according to the researchers' emphasis on different performance indicators. In this paper, we pay more attention to the optimization of SMA, so q1 is 0.6, q2 and q3 are 0.2. In summary, the objective function is established as follows

$$J_{\min}(g, \tau) = q_1 J_1 + q_2 J_2 + q_3 J_3 \quad (22)$$

where J_1 is the root-mean-square (RMS) value of SMA, J_2 is the root-mean-square value of SWS, and J_3 is the root-mean-square value of DTD. q_1, q_2, and q_3 are weight coefficients.

B. OPTIMIZATION

The Particle swarm optimization algorithm is an evolutionary computing technology based on the swarm intelligence method [24]. It was originally used to deal with continuous optimization problems, and now its application has been extended to combinatorial optimization problems. In this paper, the optimization of the objective function is mainly divided into six steps.

Step1. Define the parameters. Amount of time delay $\tau \in [0, 1]$, the feedback gain is $g \in [-170, 170]$.

Step2. Initialize the particle. Randomly generate 50 particles, namely the initial population, and set the number of iterations as $N = 100$, learning factor $c_1 = 2.2$ $c_2 = 2.2$, inertia weight $w = 0.6$, and in order to improve the search process of the PSO algorithm, the search space converges quickly to a region, the convergence factor $k = 0.729$ is added. At the same time, the convergence factor can improve the global search ability of the algorithm [25].

Step3. Calculate the fitness value. The fitness function expressed in (22) was calculated. By continuously optimizing
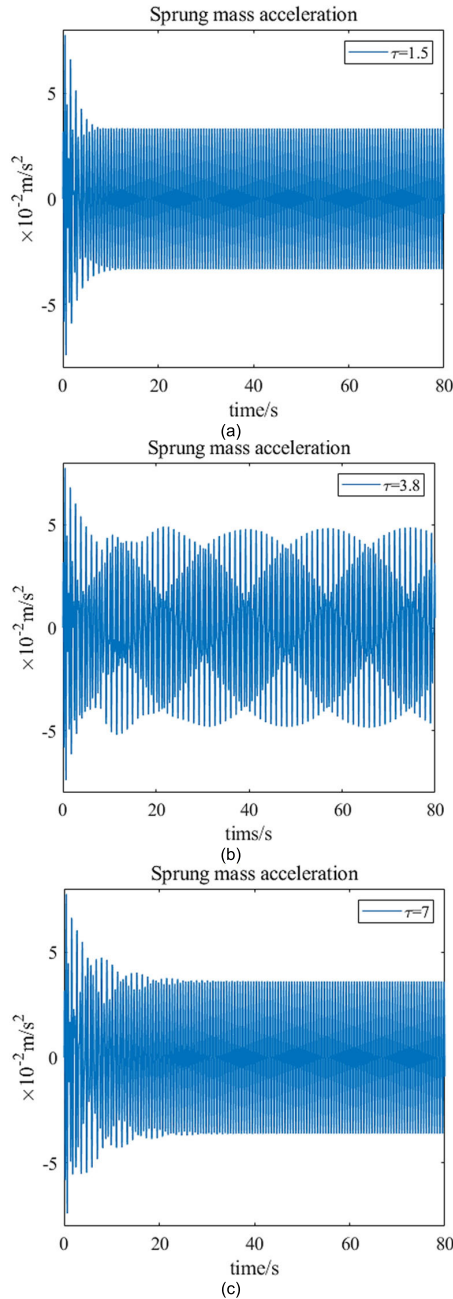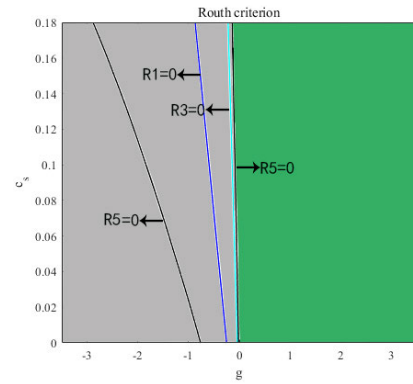
FIGURE 2. Simulation results.

FIGURE 3. Routh-Hurwitz stability criterion region.

TABLE 3. Symbol of discriminant sequence with time-delay feedback.

Region	d_0	d_1	d_2	d_3	d_4	d_5	d_6	D_1	D_2	D_3	D_4	D_5	D_6	D_7	D_8	$l-2k$
S1	+	+	-	-	-	+	+	1	1	1	-1	1	1	-1	1	0
S2	+	+	+	-	-	+	+	1	1	1	1	-1	1	-1	1	0
S3	+	+	-	-	-	-	+	1	1	1	-1	1	1	1	1	4
S4	+	+	+	-	-	-	+	1	1	1	1	-1	1	1	1	4
S5	+	+	+	+	-	-	+	1	1	1	1	1	-1	1	1	4
S6	+	+	+	+	-	-	+	1	1	1	1	1	-1	1	1	4

where k is the convergence factor,

$$\varphi = c_1 + c_2 \tag{24}$$

$$k = \frac{2}{\left|2 - \varphi - \sqrt{\varphi^2 - 4 \cdot \varphi}\right|} = 0.7 \tag{25}$$

Step5. The position of the particle updated in step.4 is substituted into the objective function to calculate the fitness value again. The fitness value of each particle is compared in the process of iterative optimization, and the particles with smaller adaptive functions are retained.

Step6. (23) is used again to update the position and velocity of particles to determine whether the conditions are met. If not, the cycle continues to iterate.

In this paper, the damping c_s of the experimental equipment used in the experiment is 7.5 N·s·m^{-1}. Under the harmonic excitation of 0.015sin(11t), the optimization parameter is τ =0.02541s, g=102N·s/m, this value is in the S6 part of the stability region, the stability switch will occur in this region, where the polynomial $F(\omega_0)$ has two distinct positive real roots, ω_1 =0.3763 and ω_2 =0.7346, satisfying $\dot{F}(\omega_1) < 0$ and $\dot{F}(\omega_2) > 0$ respectively, using equation (21), the corresponding critical delay is $\tau_{1,0} = 0.6717, \tau_{1,1} = 2.7734, \tau_{2,0} = 0.3231, \tau_{2,1} = 1.4134$.

Then order them, $\tau_{2,0} < \tau_{1,0} < \tau_{2,1} < \tau_{1,1} < \ldots$, when $\tau \in [0, \tau_{2,0})$, the system is stable, when $\tau \in [\tau_{2,0}, \tau_{1,0})$, the system becomes unstable, and when $\tau \in [\tau_{1,0}, \tau_{2,1}]$, the system becomes stable again.

And under the random excitation, the optimization parameter is $\tau = 4.2537 \times 10^{-4}$, g $= 86N \cdot s/m$. The value is also in the S6 region, The two distinct real roots of the polynomial are ω_1 =0.4180 and ω_2 =1.1411, and the stability switch is the same as above.
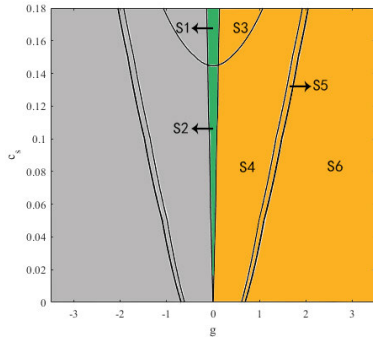
the feedback gain g and the time-delay τ, the minimum value of the fitness function is obtained. At this point, it can be considered that J is the objective function $J(K) = q_1 J_1 + q_2 J_2 + q_3 J_3$ of $K = [g, \tau]$, *pbest* and *gbest* are finally obtained.

Step4. Particle position, velocity update. Using the position update formula, and speed update formula.

$$\begin{cases} v_{id}^{k+1} = k[wv_{id}^k + c_1 rand_1^k(pbest_{id}^k - x_{id}^k) \\ \quad + c_2 rand_2^k(gbest_{id}^k - x_{id}^k)] \\ x_{id}^{k+1} = x_{id}^k + v_{id}^{k+1} \end{cases} \tag{23}$$

FIGURE 4. Time-delay independent stability regions.
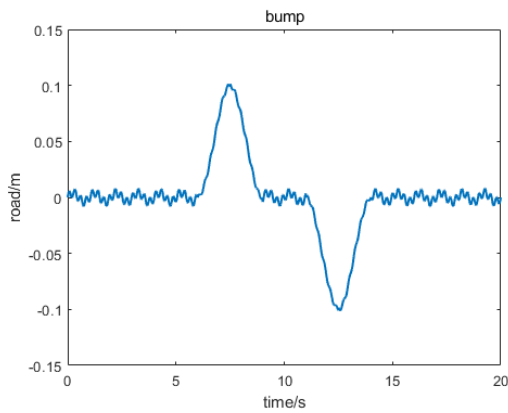
FIGURE 5. Bump excitation.

TABLE 4. Numerical simulation parameter.

Parameters	Physical meaning	Numerical value	Unit
m_b	Body mass	345	kg
m_t	Tire mass	40.5	kg
k_b	Suspension stiffness	17000	N/m
kt	Tire stiffness	192000	N/m
c_b	Suspension damping	1500	N·s/m
c_t	Tire damping	150	N·s/m
x_r	Road excitation	-	-

C. SIMULATION COMPARISON OF VEHICLE PARAMETERS

In order to preliminarily verify the vibration reduction effect of the time-delay feedback control, after completing the corresponding stability analysis and parameter optimization, we use bump excitation to compare the time-delay feedback control with the passive control in the numerical simulation. Parameters are shown in Table 4.

Numerical simulation results in Fig.5 show that under time-delay feedback control, SMA can still be comprehensively better than the uncontrolled passive suspension when passing the impact of the road surface. However, the damping effect needs to be discussed separately in SWS. The effect of time-delay control is slightly worse when passing general disturbance, but it can still achieve a better damping effect than passive suspension in the shock stage. Considering that the three ride comfort indicators are mutually restrictive and the relationship between one and the other, we think this is acceptable. And in DTD, time-delay feedback control is also superior to passive suspension.
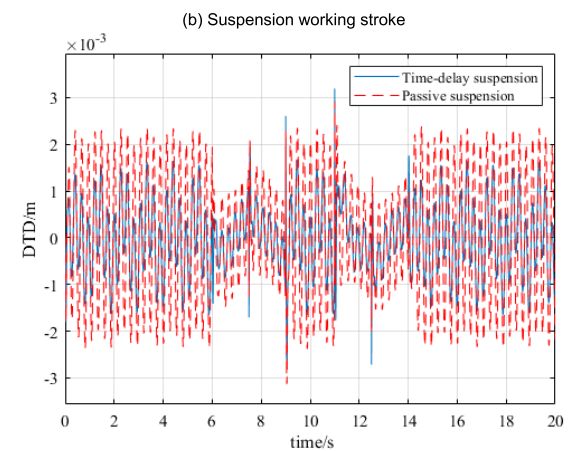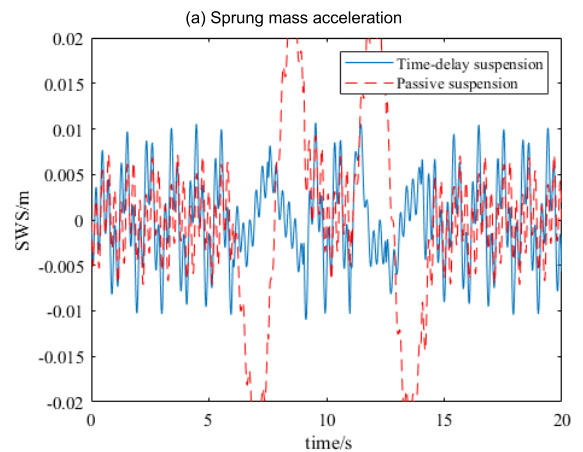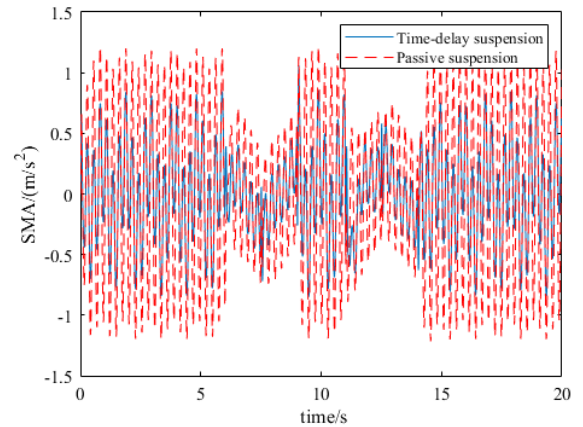

(a) Sprung mass acceleration

(b) Suspension working stroke

(c) Dynamic tire displacement

FIGURE 6. Simulation results of real vehicle parameters.

From Table 5, we can see that the three ride performance indexes of time-delay control active suspension are all better than passive suspension, among which, SMA decreases by 44.4% and SWS decreases by 50%.

V. EXPERIMENT AND SIMULATION ANALYSIS

A. THE EXPERIMENTAL EQUIPMENT

ASE(Active Suspension Experiment) equipment of Quanser Company in Canada was taken as the experimental platform, as shown in Fig.6. The device consists of three layers of
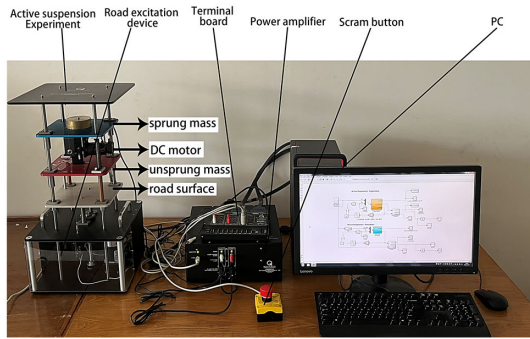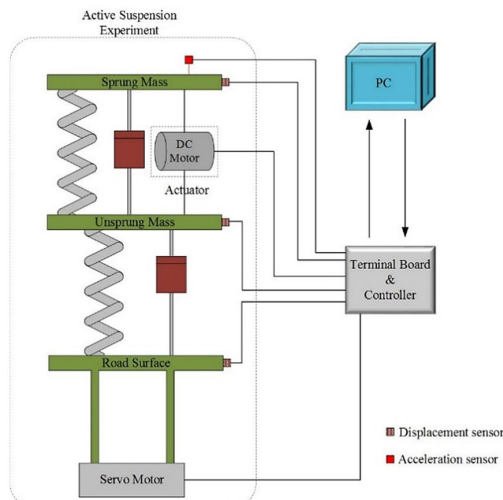
FIGURE 7. Experimental system of time-delay suspension.
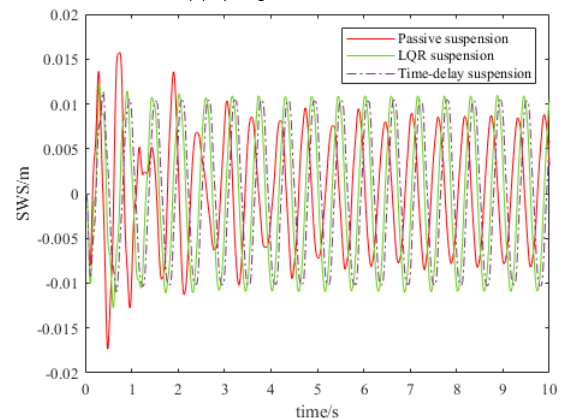

FIGURE 8. Experimental control program.

TABLE 5. RMS value of performance index under bump excitation of vehicle parameter.

| Performance Index	Passive suspension (PS)	Time-delay suspension	Drop rate
SMA (m/s²)	0.0696	0.0387	44.40%
SWS(m)	0.0048	0.096	50.00%
DTD(m)	0.0025	0.0014	44.00%

mass plates, the top plate representing the sprung mass, suspended from the middle plate by two springs. A capstan-driven DC motor is located between the top and middle plate to simulate the mount as the power mechanism. The ADXL210E biaxial acceleration sensor is installed on the top plate to measure the vertical acceleration of the car body. The middle plate and the bottom plate are the unsprung mass and the road surface. The bottom plate is connected to a fast-responding DC motor. When the motor rotates, the torque generated on the output shaft is converted into a linear force to make the bottom plate move through the lead screw and the transmission mechanism to simulate different road profiles. The controller is designed by MATLAB/Simulink on PC, and then the program is input into the internal board to control the experimental device. A brief description of the control process of the whole experiment is given in Fig.7.
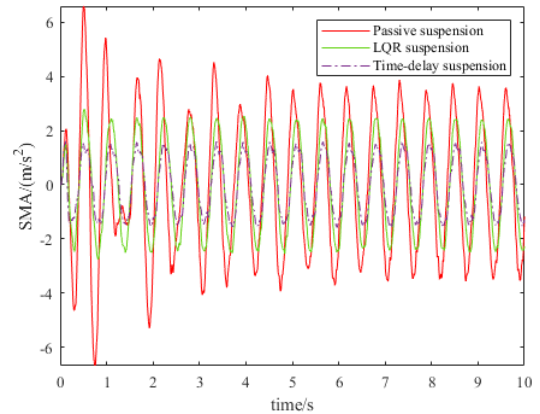
(a) Sprung mass acceleration

(b) Suspension working stroke
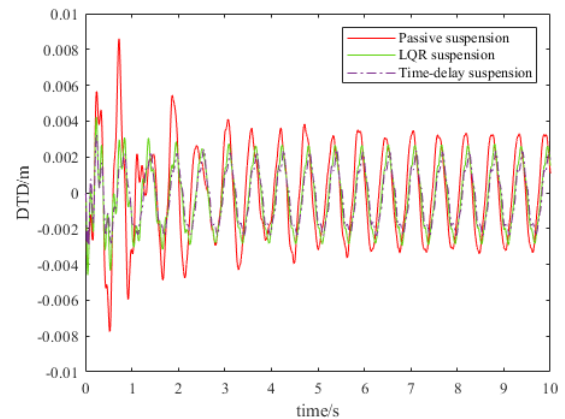
(c) Dynamic tire displacement

FIGURE 9. Comparison of experimental results of simple harmonic excitation.

B. LQR ACTIVE SUSPENSION

The linear quadratic regulator is a very mature and widely used optimal control law with linear state feedback, which can take into account both robustness and rapidity [26]. In order to make the delay feedback control have a reference comparison, this paper uses the LQR control strategy based on the state space method as the comparison. The system can be expressed in terms of the following state space:

$$\begin{cases} \dot{x} = Ax + Bu \\ y = Cx + Du \end{cases} \qquad (26)$$

TABLE 6. RMS value of performance index under harmonic excitation in the experiment.

Performance Index	Passive suspension (PS)	LQR suspension	Compared to PS drop rate	Time-delay suspension	Compared to PS drop rate
SMA (m/s²)	2.5265	1.7437	30.98%	1.0606	58.02%
SWS(m)	0.0062	0.0066	-6.452%	0.0064	-3.226%
DTD(m)	0.0025	0.0018	28.00%	0.0015	40.00%

The system status variable, input variable, and output variable are $x = [z_s - z_{us}, \dot{z}_s, z_{us} - z_r, \dot{z}_{us}]^T$, $u = [\dot{z}_r, F_c]^T$, $y = [z_s - z_{us}, \ddot{z}_s]^T$. Therefore, the four matrices of A, B, C, and D are as follows:

$$A = \begin{bmatrix} 0 & 1 & 0 & -1 \\ -\frac{k_s}{m_s} & -\frac{c_s}{m_s} & 0 & \frac{c_s}{m_s} \\ 0 & 0 & 0 & 1 \\ -\frac{k_s}{m_s} & -\frac{c_s}{m_s} & 0 & \frac{c_s}{m_s} \end{bmatrix} \quad (27)$$

$$B = \begin{bmatrix} 0 & 0 \\ 0 & \frac{1}{m_s} \\ -1 & 0 \\ \frac{c_{us}}{m_{us}} & -\frac{1}{m_{us}} \end{bmatrix} \quad (28)$$

$$C = \begin{bmatrix} 1 & 0 & 0 & 0 \\ -\frac{k_s}{m_s} & -\frac{c_s}{m_s} & 0 & \frac{c_s}{m_s} \end{bmatrix} \quad (29)$$

$$D = \begin{bmatrix} 0 & 0 \\ 0 & \frac{1}{m_s} \end{bmatrix} \quad (30)$$

Define quadratic performance index function,

$$J = \int_0^\infty x(t)'Qx(t) + RF_c(t)^2 dt \quad (31)$$

The problem of taking the minimum value is the optimal control problem, and the optimal control force is $F_c = -Kx$. The weighting matrix of state variables and control variables is selected as follows:

$$Q = \begin{bmatrix} 450 & 0 & 0 & 0 \\ 0 & 30 & 0 & 0 \\ 0 & 0 & 5 & 0 \\ 0 & 0 & 0 & 0.01 \end{bmatrix}, R = 0.01.$$

Finally, invoking the LQR toolbox in MATLAB, the basic format is $(K.S.E) = LQR(A, B, Q, R, N)$, the program is built in Simulink, and the optimal control gain matrix is $K = \begin{bmatrix} 22.6964 & 48.7139 & 3.7933 & 3.8516 \end{bmatrix}$.

C. HARMONIC EXCITATION

To verify the vibration reduction performance of time-delay feedback active suspension, the parameters obtained by harmonic excitation and optimization were put into the system for simulation and experimental verification. The experimental results were compared with passive uncontrolled suspension and LQR active suspension respectively. The root-mean-square(RMS) values of sprung mass acceleration(SMA), suspension working stroke(SWS), and dynamic
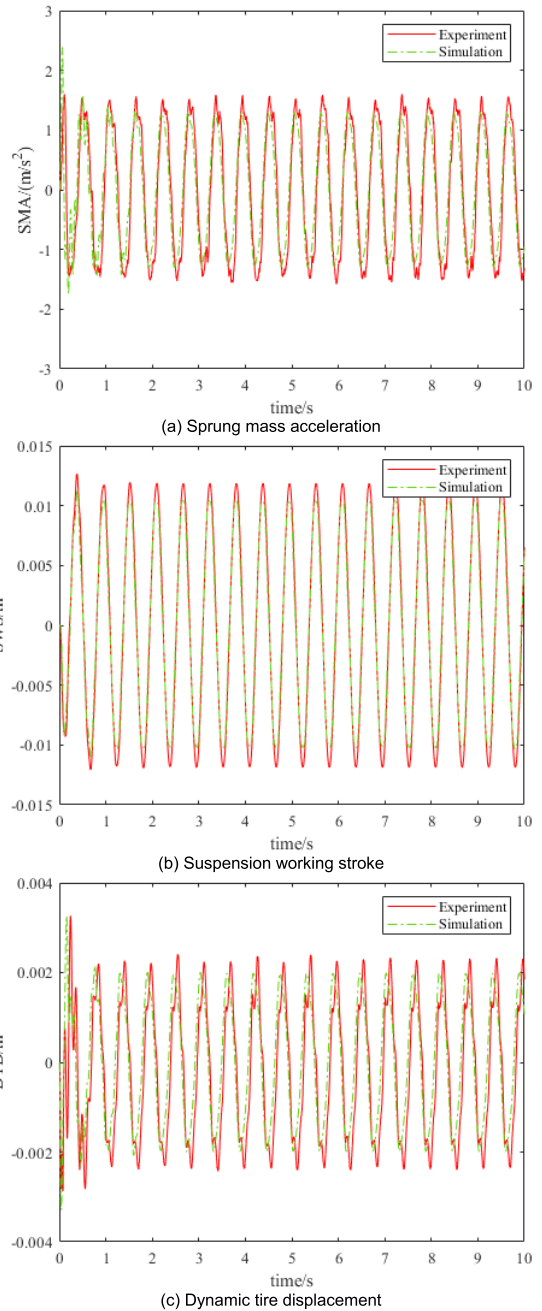

(a) Sprung mass acceleration

(b) Suspension working stroke

(c) Dynamic tire displacement

FIGURE 10. Comparison between experiment and simulation of timedelay suspension under harmonic excitation.

tire displacement(DTD) are taken as the evaluation indexes. The experimental results are shown in Fig.8. The values of each performance index are shown in Table.6.

According to Fig.8 and Table.6, compared with the passive suspension, the RMS values of SMA, SWS, and DTD of the LQR active suspension decreased by 30.98%, −6.452%, and 28%, respectively. Meanwhile, the suspension based on the feedback of body speed time-delay decrease ranges reached 58.02%%, -3.226%, and 40% respectively. Although the suspension dynamic travel increased due to the contradiction between the three indexes, it still did not reach the upper limit
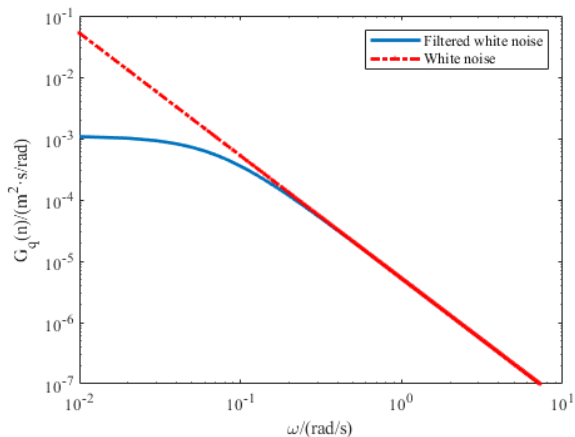
FIGURE 11. Road surface power spectral density contrast curve in double log coordinate.

of 0.038m, so there would be no limit impact. Meanwhile, time-delay active suspension compared with LQR active suspension, as the most important index of ride comfort, the RMS of SMA dropped from 1.7437 to 1.0606, the decrease rate reached 39.18%, and the RMS values of SWS and DTD also improved slightly.

By observing Fig.9, it can be seen that there are some errors in the experimental and simulation results under the time-delay feedback control. The RMS of the simulation values of the three performance indexes are 0.9279, 0.0083, and 0.0014, respectively. Compared with the experimental results in Table 4, the errors are 12.51%, 12.16%, and 7.13%, but the errors are within 15%, it can be shown that there is good consistency.

D. RANDOM EXCITATION
1) RANDOM EXCITATION MODEL

In the theoretical analysis related to automobile vibration, the internationally recognized road surface power spectral density is generally used to describe the statistical characteristics of road roughness, that is, the white noise road surface spectrum represented by the frequency of road excitation circle [27]:

$$G_q(\omega) = \frac{2\pi v G_q(n_0) n_0^2}{\omega^2} \tag{32}$$

where v is the driving speed, n_0 is the reference spatial frequency, $n_0 = 0.1\text{m}^{-1}$; $G_q(n_0)$ is the road surface power spectral density at the reference spatial frequency n_0, namely, the road roughness coefficient.

However, when ω tending to 0, the (32) tends to infinity, It's impossible for a road surface in a real environment, so white noise can't reflect real roughness in the low-frequency range of the road surface spectrum. In this case, the lower cut-off frequency ω_0 is introduced. When the frequency is lower than that ω_0, the spectral density amplitude of the road surface can be kept constant. In this way, the road surface input model can

(a) Sprung mass acceleration

(b) Suspension working stroke
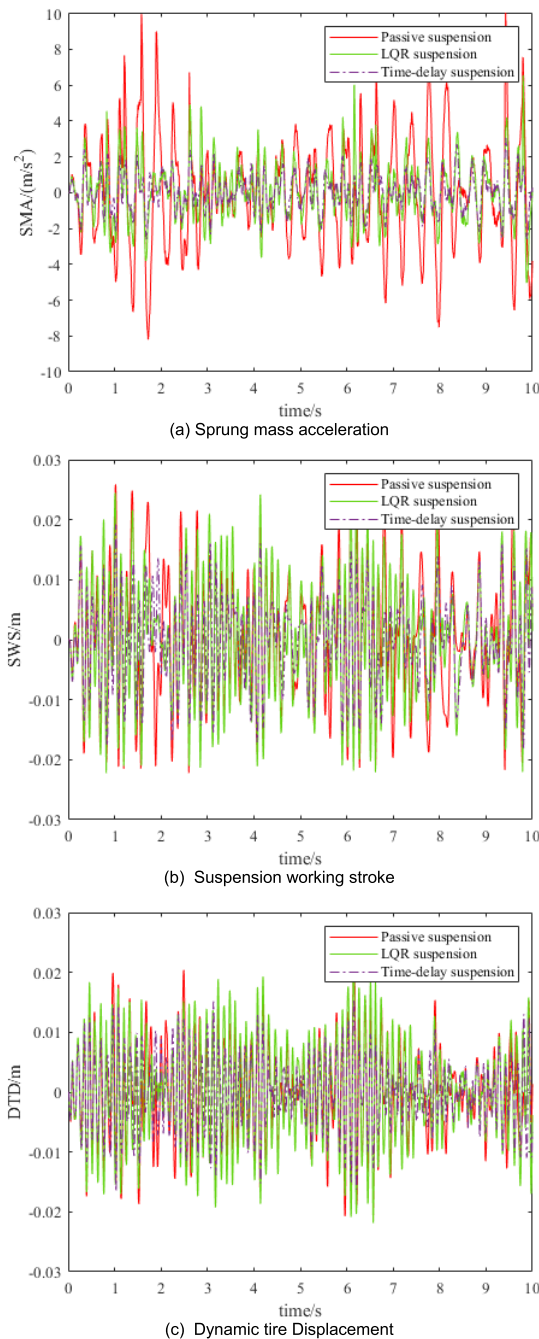

(c) Dynamic tire Displacement

FIGURE 12. Comparison of experimental results of random excitation.

be expressed in the form of filtered white noise [28]:

$$G_q(\omega) = \frac{2\pi v G_q(n_0) n_0^2}{\omega^2 + \omega_0^2} \tag{33}$$

where, $\omega_0 = 2\pi v n_{00}$, $n_{00} = 0.011\text{m}^{-1}$ is the lower cut-off frequency in space. By synthesizing equations (32) and (33), the road surface power spectrum obtained under the class B road surface and speed of 60km/h is shown in Fig.10.

In double logarithmic coordinates, the white noise road surface spectrum curve is an oblique line with a slope of approximately -2:1. However, the filtered white noise road
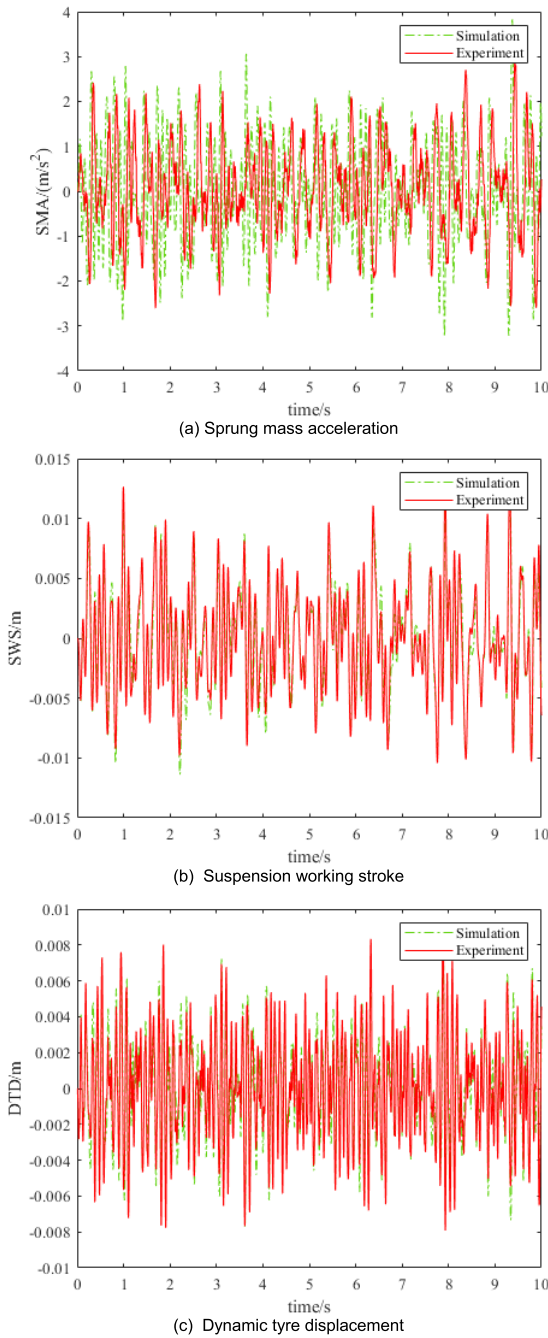
FIGURE 13. Comparison between experiment and simulation of time-delay suspension under random excitation.

surface spectrum is a smooth curve whose slope approximately changes from 0:1 to -2:1. This shows that compared with filtering white noise, noise is overestimated when representing road roughness, and filtering white noise can more truly reflect road roughness.

2) RANDOM EXCITATION EXPERIMENT VERIFICATION

To further verify the vibration reduction effect of the time-delay feedback suspension, the optimization parameters and the road excitation expressed in equations (33) are substituted.

TABLE 7. RMS value of performance index under random excitation in the experiment.

Performance Index	Passive suspension (PS)	LQR suspension	Compared to PS drop rate	Time-delay suspension	Compared to PS drop rate
$SMA(m/s^2)$	3.3669	1.5891	52.80%	1.0250	69.56%
$SWS(m)$	0.0077	0.0074	3.900%	0.0069	10.39%
$DTD(m)$	0.0057	0.0060	-5.260%	0.0055	3.510%

According to the results in Fig.11 and Table.7, the sprung mass vertical acceleration, suspension dynamic travel, and tire dynamic displacement of LQR active suspension under random excitation decreased by 52.80%, 3.900%, and -5.260% compared with passive suspension, meanwhile, the suspension under time-delay feedback control decreased by 69.56%, 10.39%, and 3.510% respectively compared with passive suspension. The optimization amplitude is significantly improved. Meanwhile, compared with LQR active suspension, the three indexes of time-delay feedback suspension are decreased by 35.50%, 6.76%, and 8.33%, respectively.

It can be seen from Fig.12 that under random excitation, the time-delay suspension based on body speed feedback has a good consistency in simulation and experiment, the experimental value of the RMS of the SMA is 1.0250, slightly less than the simulation value 1.1807. This is because for random excitation when the active time-delay is large, the data acquisition and transmission process of the test system is relatively complex. Although the error is slightly larger than 15.57%, the general engineering error is allowed to be 20% or even higher [29], so it can still meet the engineering requirements.

VI. CONCLUSION

In this paper, a 2-DOF time-delay feedback suspension is taken as the research object, and the vibration reduction performance under time-delay feedback control is studied by combining theoretical, numerical, and experimental methods, the following conclusions are obtained:

(1) According to the 2-DOF time-delay suspension model based on sprung mass speed feedback, the stability region of the system is analyzed by using the Routh-Hurwitz criterion and Sturm polynomial discriminant theorem. With the increase of suspension damping, the time-delay independent stability region increases.

(2) Compared with the passive suspension without control, LQR active suspension can obtain a good vibration reduction effect. The RMS value of SMA decreases from 2.5265 to 1.7437 under harmonic excitation by 31%, and from 3.3669 to 1.5891 under random excitation by 52.8%. However, its optimal control performance completely depends on the weighting coefficient of state variables and input variables, the weighting coefficient is mostly determined by trial algorithm [30] at home and abroad, which cannot include the influence of road excitation and has

strong subjectivity, so it has certain limitations. At the same time, because the relationship between the three ride comfort indexes is mutually restricted, there is a situation that the SWS or DTD slightly increases while the SMA is optimized.

(3) The experimental results show that the suspension vibration reduction performance under time-delay feedback control has a certain range of optimization compared with the LQR control active suspension. Under harmonic excitation, the RMS value of SMA decreases from 1.7437 to 1.0606 by 39.17%, while under random excitation it decreases from 1.5891 to 1.0250 by 35.5%. And in the simulation and experimental comparison under the same working condition, the error of RMS of SMA is 12.51% and 15.57% respectively, which meet the engineering requirements.

The essence of time-delay feedback control is the two-parameter control method of feedback gain and time-delay amount, the two physical parameters can be adjusted independently so that the controlled system has a wide design space. But by comparing the simulation results of time-delay feedback control, we can find the vibration damping performance in the experimental results is somewhat reduced. This is because the suspension system is nonlinear in reality, the nonlinear characteristics of the suspension system are not considered in the modeling process, however, the experiment of nonlinear and time-delay joint control system is more difficult. Meanwhile, as a suspension system under time-delay feedback control, it's not just about improving the algorithm, the redundant design when the amount of time-delay is not optimal should also be considered. For example, how to match the damping coefficient and stiffness better so that the vibration is still within the acceptable range under the non-optimal time delay, all of the above issues are difficult points that we should focus on in our future research. Finally, the vibration problem of the system with time-delay studied in this paper belongs to the system with a small time-delay, if the active suspension with time-delay control wants to be further applied to the actual vehicle, it should also explore the change of ride comfort index under the condition of large time-delay, because the suppression of vibration with time delay is not monotonous change, and the input of large time delay to the system is very likely to worsen the vibration control effect of the system, which is a problem to be solved in the future.

REFERENCES

[1] T. H. Langer, M. K. Ebbesen, and A. Kordestani, "Experimental analysis of occupational whole-body vibration exposure of agricultural tractor with large square baler," *Int. J. Ind. Ergonom.*, vol. 47, pp. 79–83, May 2015.

[2] R. P. Blood, J. D. Ploger, M. G. Yost, R. P. Ching, and P. W. Johnson, "Whole body vibration exposures in metropolitan bus drivers: A comparison of three seats," *J. Sound Vibrat.*, vol. 329, no. 1, pp. 109–120, Jan. 2010.

[3] L. M. Roseiro, M. A. Neto, A. M. Amaro, C. J. Alcobia, and M. F. Paulino, "Hand-arm and whole-body vibrations induced in cross motorcycle and bicycle drivers," *Int. J. Ind. Ergonom.*, vol. 56, pp. 150–160, Nov. 2016.

[4] F. Chi, J. Zhou, Q. Zhang, Y. Wang, and P. Huang, "Avoiding the health hazard of people from construction vehicles: A strategy for controlling the vibration of a wheel loader," *Int. J. Environ. Res. Public Health*, vol. 14, no. 3, p. 275, Mar. 2017.

[5] M. Bovenzi and C. T. J. Hulshof, "An updated review of epidemiologic studies on the relationship between exposure to whole-body vibration and low back pain (1986–1997)," *Int. Arch. Occupational Environ. Health*, vol. 72, no. 6, pp. 351–365, Sep. 1999.

[6] D. Koradecka, *Handbook of Occupational Safety and Health*. New York, NY, USA: Taylor & Francis, 2010.

[7] G. Wang, L. Gu, and F. Sun, "Current status and tendency of development in vehicle active suspension," *Acta Armamentarii*, pp. 80–83, 2000.

[8] S. G. Prassad and M. Mohan, "A contemporary adaptive air suspension using LQR control for passenger vehicles," *ISA Trans.*, vol. 93, pp. 244–254, Oct. 2019.

[9] J. J. Robert, P. S. Kumar, S. T. Nair, D. H. S. Moni, and B. Swarneswar, "Fuzzy control of active suspension system based on quarter car model," *Mater. Today, Proc.*, vol. 66, pp. 902–908, 2022.

[10] F. Wang, J. Zhou, and C. Ren, "Research on chaotic dynamics properties for nonlinear suspension system with time-delay," *Chin. J. Appl. Mech.*, vol. 33, no. 5, pp. 891–897, 2016.

[11] N. Olgac and B. T. Holm-Hansen, "A novel active vibration absorption technique: Delayed resonator," *J. Sound Vibrat.*, vol. 176, no. 1, pp. 93–104, Sep. 1994.

[12] C. Chen, J. Xiong, Z. Wan, J. Lei, and K. Zhang, "A time delay compensation method based on area equivalence for active damping of an LCL-type converter," *IEEE Trans. Power Electron.*, vol. 32, no. 1, pp. 762–772, Jan. 2017.

[13] G. I. Koumene Taffo, M. Siewe Siewe, and C. Tchawoua, "Stability switches and bifurcation in a two-degrees-of-freedom nonlinear quarter-car with small time-delayed feedback control," *Chaos, Solitons Fractals*, vol. 87, pp. 226–239, Jun. 2016.

[14] H. Qi, J. Xu, and M. Fang, "Time-delayed feedback control of flutter for supersonic airfoils," *Appl. Math. Mech.*, vol. 37, no. 2, pp. 210–218, 2016.

[15] Q. Ye, G. Chaojun, R. Wang, C. Zhang, and Y. Cai, "Stability analysis of the anti-lock braking system with time delay," *Proc. Inst. Mech. Eng., I, J. Syst. Control Eng.*, vol. 236, no. 4, pp. 671–682, Apr. 2022.

[16] S. Shao, C. Ren, and D. Jing, "Vibration control of nonlinear active suspension system with time delay," *Chin. J. Appl. Mech.*, vol. 38, no. 3, pp. 1218–1225, 2021.

[17] S. Zhou, Y. Li, Z. Ren, G. Song, and B. Wen, "Nonlinear dynamic analysis of a unilateral vibration vehicle system with structural nonlinearity under harmonic excitation," *Mech. Syst. Signal Process.*, vol. 116, pp. 751–771, Feb. 2019.

[18] L. Chen, R. Wang, H. Jiang, L. Zhou, and S. Wang, "Time delay on semi-active suspension and control system," *Chin. J. Mech. Eng.*, vol. 42, no. 1, pp. 130–133, 2006.

[19] T. Vyhlídal, J. Anderle, J. Bušek, and S.-I. Niculescu, "Time-delay algorithms for damping oscillations of suspended payload by adjusting the cable length," *IEEE/ASME Trans. Mechatronics*, vol. 22, no. 5, pp. 2319–2329, Oct. 2017.

[20] G. Yan, M. Fang, and J. Xu, "Analysis and experiment of time-delayed optimal control for vehicle suspension system," *J. Sound Vibrat.*, vol. 446, pp. 144–158, Apr. 2019.

[21] D. Crolla and F. Yu, *Vehicle Dynamics and Control*. People's Communications Publishing House, 2004.

[22] Z. H. Wang and H. Y. Hu, "Stability switches of time-delayed dynamic systems with unknown parameters," *J. Sound Vibrat.*, vol. 233, no. 2, pp. 215–233, Jun. 2000.

[23] S. Shao, C. Ren, D. Jing, and T. Yan, "Stability, bifurcation and chaos of nonlinear active suspension system with time delay feedback control," *J. Vibr. Shock*, vol. 40, pp. 281–290, 2021.

[24] L. Sun, X. Song, and T. Chen, "An improved convergence particle swarm optimization algorithm with random sampling of control parameters," *J. Control Sci. Eng.*, vol. 2019, Jun. 2019, Art. no. 7478498.

[25] I. Abd Latiff and M. O. Tokhi, "Fast convergence strategy for particle swarm optimization using spread factor," in *Proc. IEEE Congr. Evol. Comput.*, May 2009, pp. 2693–2700.

[26] G. Li, R. Gu, R. Xu, G. Hu, N. Ouyang, and M. Xu, "Study on fuzzy LQG control strategy for semi-active vehicle suspensions with magnetorheological dampers," *Noise Vib. Control*, vol. 41, no. 4, pp. 129–136, 2021.

[27] Z. Yu, *Automobile Theory*, 2nd ed. Beijing, China: China Machine Press, 1990.

[28] F. Yu and Y. Lin, *Vehicle System Dynamics*. Beijing, China: China Machine Press, 2005.

[29] J. Yang, J. Wang, and G. Wang, "Analysison the effect of marine propulsion shafting alignment on its vibration," *J. Dyn. Control*, vol. 14, no. 2, pp. 157–164, 2016.

[30] P. Brezas, M. C. Smith, and W. Hoult, "A clipped-optimal control algorithm for semi-active vehicle suspensions: Theory and experimental evaluation," *Automatica*, vol. 53, pp. 188–194, Mar. 2015.

YANG NAN was born in Dongying, Shandong, China. He is currently pursuing the master's degree in vehicle engineering system dynamics with the Shandong University of Technology. From 2017 to 2018, he participated in the Formula College of China Competition and the Honda Energy Saving Cup Competition as a member of the Car Design Team.

SUJUAN SHAO was born in Dezhou, Shandong, China, in 1989. She received the B.E. degree in mechanical design manufacture and automation from Zaozhuang University, Zaozhuang, China, in 2012, the M.E. degree in mechanical design and theory from the East China University of Science and Technology, Shanghai, China, in 2015, and the Ph.D. degree in mechanical engineering from the Shandong University of Technology, Zibo, China.

Since 2021, she has been a Lecturer with the School of Transportation and Vehicle Engineering, Shandong University of Technology. Her current research interests include nonlinear dynamics, time-delay damping, and noise and vibration control.

CHUANBO REN was born in Weifang, Shandong, China, in 1964. He received the B.E. degree in mechanical manufacturing and technology from the Shandong Institute of Agricultural Mechanization, Zibo, China, in 1984, the M.E. degree in solid mechanics from the Jiangsu University of Science and Technology, Zhenjiang, China, in 1989, and the Ph.D. degree in structural mechanics from the Dalian University of Technology, Dalian, China, in 1997.

From 1986 to 1994, he was a Lecturer with the College of Automotive Engineering, Shandong University of Technology. From 1997 to 2001, he was a Professor with the College of Automotive Engineering, Shandong University of Technology. Since 2001, he has been a Professor with the School of Transportation and Vehicle Engineering, Shandong University of Technology. His current research interests include linear and nonlinear dynamics with time delay, structural mechanics, and automobile vibration reduction and optimization.

KAIWEI WU received the master's degree in engineering from the Shandong University of Technology, in 2021, where he is currently pursuing the Ph.D. degree in engineering. He has published academic articles as the first author, two of which were indexed by SCI. He participated in the competition of the National Natural Science Foundation. He won the honorary titles of "Excellent Student of the University" and "Honor Student of Transportation College" for two consecutive years. His postgraduate research achievements won the Third Prize of Excellent Postgraduate Achievement of Shandong Province. He is a Reviewer of the *Journal of the Brazilian Society of Mechanical Sciences and Engineering* and *Proceedings of the Institution of Mechanical Engineers—D: Journal of Automotive Engineering*.

YAJIE CHENG was born in Suzhou, Anhui, China. She is currently pursuing the master's degree in vehicle engineering system dynamics with the Shandong University of Technology. She has published articles in several SCI journals. She has made outstanding achievements in the direction of time-delay vibration suspension.

PENGCHENG ZHOU was born in Jining, Shandong, China. He is currently pursuing the master's degree in vehicle engineering system dynamics with the Shandong University of Technology, with a focus on the trajectory control of autonomous vehicles. He has published articles in several high-level English journals. He has made outstanding achievements in the four-wheel steering direction.

● ● ●